Humbla, Stefan; Kaleem, Saqib; Müller, Jens; Rentsch, Sven; Stephan, Ralf; Stöpel, Dirk; Vogt, Gabor; Hein, Matthias:

On-orbit verification of a 4 × 4 switch matrix for space applications based on the low temperature co-fired ceramics technology

URN: urn:nbn:de:gbv:ilm1-2015210245

Published OpenAccess: January 2015

Original published in:

Frequenz : journal of RF-engineering and telecommunications. - Berlin : De Gruyter (ISSN 2191-6349). - 66 (2012) 11/12, S. 355-362.
DOI: 10.1515/freq-2012-0106
URL: http://dx.doi.org/10.1515/freq-2012-0106
[Visited: 2015-01-14]

DOI 10.1515/freq-2012-0106 — Frequenz 2012; 66(11-12): 355–362

Stefan Humbla*, Saqib Kaleem, Jens Müller, Sven Rentsch, Ralf Stephan, Dirk Stöpel, Gabor Vogt and Matthias A. Hein

On-Orbit Verification of a 4 × 4 Switch Matrix for Space Applications based on the Low Temperature Co-fired Ceramics Technology

Abstract: We have developed a compact, high-performance, mechanically robust reconfigurable microwave switch matrix as well as peripheral components such as diode driver, voltage controlled oscillator, and power detector modules for satellite applications using the low temperature co-fired ceramics technology (LTCC) and hybrid integration of integrated circuits. In order to verify the technology for space applications, we combined these components to build a system that enables automated verification of the switch matrix in space, accounting for power consumption, mass, overall geometrical dimensions, and mechanical robustness. The system passed a full space qualification. During a one year On-Orbit-Verification (OOV) mission aboard the German test satellite TET-1 (technology evaluation carrier) launched on July 22, 2012, the correct operation and reliability of the entire switch matrix system and thereby the used technology will be demonstrated.

Keywords: ceramics, microwave switches, microwave technology, satellite communication on-board systems, switch matrix

PACS® (2010). 84.40

***Corresponding author: Stefan Humbla:** Institute for Micro- and Nanotechnologies Ilmenau University of Technology, Ilmenau, 98684, Germany, E-mail: stefan.humbla@tu-ilmenau.de
Saqib Kaleem: Institute for Micro- and Nanotechnologies Ilmenau University of Technology, Ilmenau, 98684, Germany
Jens Müller: Institute for Micro- and Nanotechnologies Ilmenau University of Technology, Ilmenau, 98684, Germany
Sven Rentsch: Institute for Micro- and Nanotechnologies Ilmenau University of Technology, Ilmenau, 98684, Germany
Ralf Stephan: Institute for Micro- and Nanotechnologies Ilmenau University of Technology, Ilmenau, 98684, Germany
Dirk Stöpel: Institute for Micro- and Nanotechnologies Ilmenau University of Technology, Ilmenau, 98684, Germany
Gabor Vogt: Institute for Micro- and Nanotechnologies Ilmenau University of Technology, Ilmenau, 98684, Germany
Matthias A. Hein: Institute for Micro- and Nanotechnologies Ilmenau University of Technology, Ilmenau, 98684, Germany

1 Introduction

In previous papers we described the design and space qualification of a reconfigurable 4×4 switch matrix module for the Ka-band downlink (17 to 22 GHz), and the satellite experiment for the on-orbit-verification mission in detail [1]–[3]. The optimisation of module size, assembly technology, and choice of materials ensured good mechanical reliability for the resulting version of the switch matrix with compact lateral dimensions of 32 mm × 30 mm.

In order to verify proper electrical function of the switch matrix module, additional components were required to generate and detect microwave signals, control the on- and off-states of the PIN-diode switch ICs, and provide digital interfaces and power supply. All building blocks were designed, manufactured and combined to compose a space experiment. After the start of the carrier rocket on July 22, 2012, from Baikonur, the system delivers measured data aboard the TET-1 satellite, to prove the space capability of the ceramic technology, by analysing the switch matrix system for one year under real operating conditions on a low earth orbit at around 500 km height. In this paper, the characterisation of material properties, the calibration process, and the analysis of the measured data are described. Additionally, developments towards more complex designs based on the multiple use of the described switch matrix module are proposed.

2 Multilayer LTCC technology

The LTCC technology is well-known for its robustness, low microwave losses, potential for hybrid integration, modular and three-dimensional design capabilities, and hermetic packaging. Together with moderate production costs and flexibility, this technology has proven its value for high-frequency applications up into the millimetre wave range. A variety of LTCC applications at RF and

microwave frequencies has emerged meanwhile [4]–[7]. Most of these applications exploit the compactness achieved by the hybrid integration of microwave components, which are often arranged at the surface of LTCC modules, with signal and bias circuitry buried in inner layers. Another important benefit is the persistency to harsh thermal and chemical environmental conditions.

At Ilmenau University of Technology, we have developed and refined a truly three-dimensional design, development, and manufacturing of ceramic multilayer modules for satellite communications at the Ka-band downlink frequency range. Possible candidate subsystems, which could benefit from the specific advantages of the LTCC technology, include power amplifier stages, frequency synthesizers, and switch matrices. These examples have in common that they would require significant volume if built from discrete components, or would cause significant costs if integrated monolithically. Together with partners of the R&D project KERAMIS-II (ceramic microwave circuits for satellite communications) funded by the German space agency on behalf of the Federal Ministry of Economics, we have developed such subsystems [8]. The compactness of the switch matrix module results in a mass reduction from 2000 g to 10 g compared to standard coaxial switch technologies.

3 Measurement of material properties

The design of microwave components requires the consideration of design rules such as the resolution limits for lines and spaces, manufacturing tolerances inherent to the screen printing process or layer misalignment, substrate heights, line thicknesses, *et cetera*. The main electrical properties of the substrate and conductor materials are the dielectric permittivity, the dielectric loss tangent, and the electrical conductivity resulting from a specific combination of starting materials and sintering conditions. While the electrical conductivity can be characterised at low frequencies, the characterisation of the dielectric properties at the frequencies of interest is more complex and therefore described in greater detail.

Among the multitude of methods to measure the dielectric permittivity of solid materials, ring resonators (RR), rectangular waveguides and split-post dielectric resonators (SPDR) are widely used. The ceramic technology requires precise processing to fit samples into waveguides for characterisation while the implementation of ring resonators into test substrates is less complicated. The use of split-post resonators allows for the characterisation of samples without metallisation, for known substrate thicknesses but at discrete frequencies only. The ring resonator resonances are distributed over frequency nearly at multiples of the fundamental resonance. Resonators on the surface of the ceramic multilayer module enable easy measurements of the geometry, which are required for the calculation of permittivity. However, the excitation of surface waves and radiation depending on the geometry and the port setup may lead to ambiguities of the measurement results. Buried resonators can be shielded more effectively and offer therefore better performance, as radiation is negligible, although at the expense of errors in geometry estimation based on ultrasonic or X-ray inspection.

The combination of different methods enables the general distinction between different types of losses over a broader frequency range, as depicted in Fig. 1 and Fig. 2 [9]. The two methods are compared for the widely used LTCC-materials DuPont 951 Green Tape™ (DP-951) which is easier to process and offers a variety of pastes and DuPont 943 Green Tape™ (DP-943) which offers lower dielectric losses. The measurements using SPDR are limited to frequencies below 25 GHz while RR are limited by the wafer prober measurement equipment used.

The results of the measurements are summarised in Table I and show qualitative agreement with the datasheet values especially as they have been given for different frequencies. The losses are more accurate for the SPDR

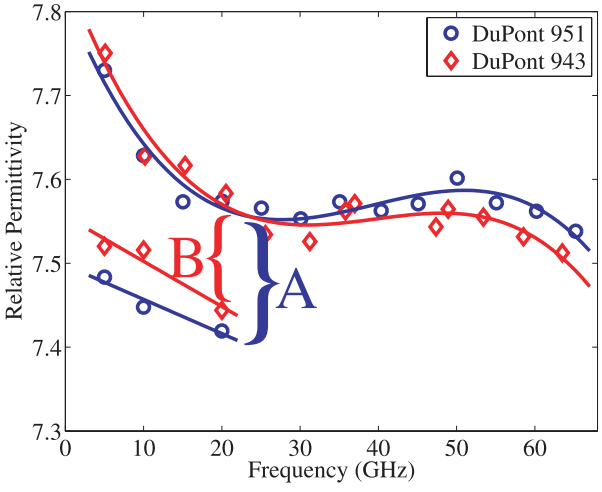

Fig. 1: Comparison of measured dielectric permittivities for the ceramic materials DuPont 943 (red diamonds and interpolated curves) and 951 Greentape™ (blue circles and curves) using ring-resonators across the entire frequency range, and split-post dielectric resonators at selected frequencies below 20 GHz. The differences A and B between the two sets of curves indicate the influence of ohmic and radiation losses.

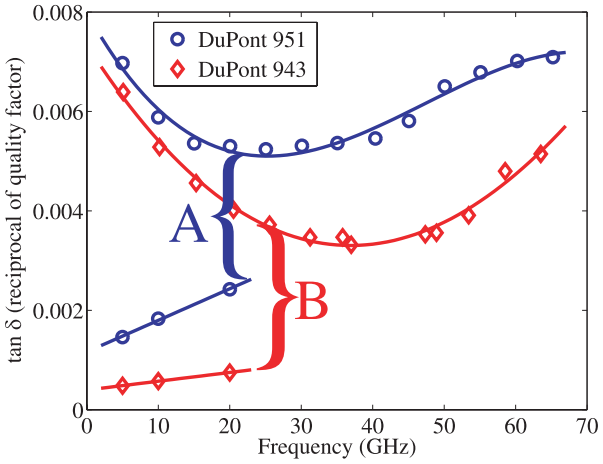

Fig. 2: Same as in Fig. 1, but for the measured losses (tan δ) for the ceramic materials DuPont 943 (red diamonds and curves) and 951 Greentape™ (blue circles and curves).

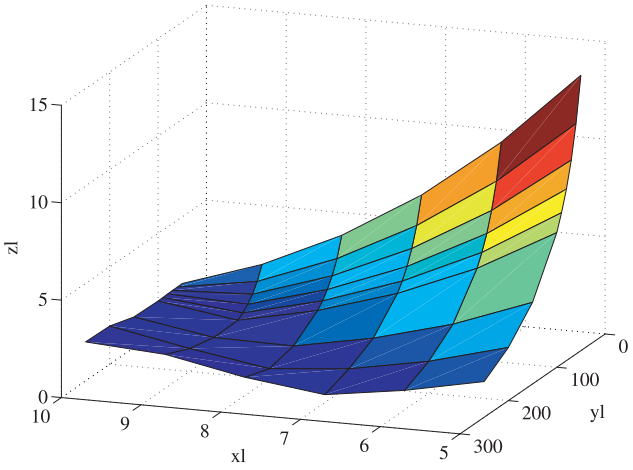

Fig. 3: Fractional variation of the line impedance of a coplanar waveguide versus dielectric permittivity of the substrate and width of the signal conductor for geometrical deviations of 5 µm, for fixed substrate height (200 µm) and impedance (50 Ω).

material/method	permittivity	effective loss tangent [10^{-3}]
DP-951 datasheet	7.8	6
DP-951 SPDR	7.42	6.06
DP-951 RR	7.57	13.0
DP-943 datasheet	7.4	2
DP-943 SPDR	7.45	1.88
DP-943 RR	7.57	10.3

Table I: Comparison of measured properties based on ring- and Split-post dielectric-resonators for the ceramic materials DP-951 and DP-943. The measured data refer to 20 GHz while the datasheet values are at 3 GHz and 40 GHz, respectively.

measurements because the ring resonators include ohmic and radiation losses, although the latter are of minor importance due to the buried and shielded transmission lines.

We found in addition, that the dielectric properties are affected by the sintering profiles in specific ways for the different material systems [10]. Especially multiple expositions to higher temperatures for the processing of post-fire prints cause a shift in permittivity. However, designs based on the values measured in this work resulted in good agreement between simulation and measurement.

4 Robust design of multilayer components

Based on the material parameters derived from measurement, designs should yield devices with measurable properties matching the design goals and numerical simulations. However, due to unavoidable manufacturing tolerances and variations, an additional geometrical process-specific deviation occurs that may affect the microwave performance, especially for filters and small structures.

One solution to minimise the influence of manufacturing tolerances is the incorporation of new structuring technologies like photo-structurable pastes and resinates [11]. This enhances resolution and reduces the relative error caused by screen printing. Another approach to increase yield can be included in the design of microwave structures. Based on the method *Design of Experiments* and *Sensitivity Analysis*, an optimisation can be performed to take advantage of existing degrees of freedom.

A simple example is the use of a coplanar waveguide structure that enables a trade-off between signal conductor width w and gaps s between signal and grounds for a given impedance and propagating mode. Fig. 3 illustrates the relative variation of the line impedance for different w and dielectric permittivities while the gaps have been set such as to keep a characteristic impedance of 50 Ω. The constant influence for all geometries is a geometrical deviation of 5 µm. As expected, the relative impedance error increases for smaller structures and can be improved by the application of larger geometries or by improving resolution and repeatability under design constraints for the required impedances.

5 The switch matrix experiment

During a one-year mission, the experiment provides data verifying the *technology readiness level* (TRL) [12] of

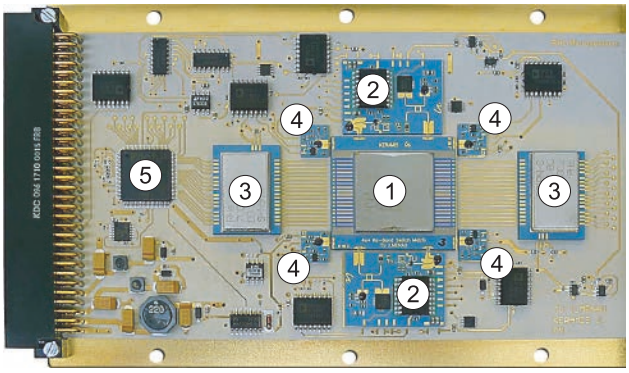

Fig. 4: Photography of the final flight model as integrated into the TET-payload. The switch matrix (1), VCO-module (2), diode driver (3), power detector (4), the digital control via FPGA (5) and peripheral components are mounted onto a RT/duroid 6002 substrate glued onto a Kovar carrier board.

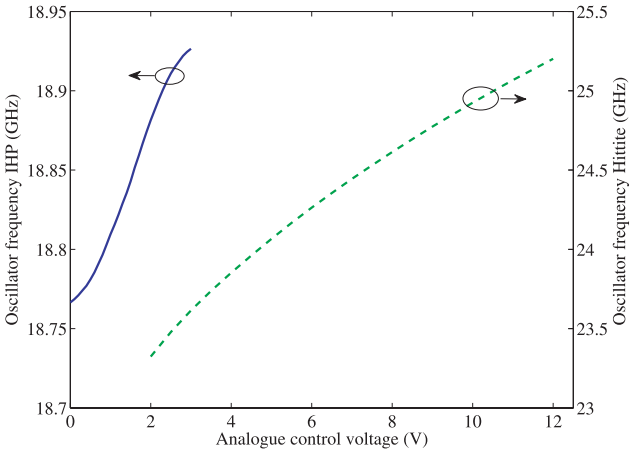

Fig. 5: Analogue tuning ranges of the two oscillators implemented in the VCO-modules. The output frequency of the IHP oscillator can be adjusted between 18.77 and 18.93 GHz (solid blue curve), and from 23.32 to 25.2 GHz for the Hittite oscillator (dashed green curve).

the ceramic multilayer technology and space qualified assembly. So far a TRL level of eight has been achieved. This verification is the basis for future work towards geostationary satellite payload components, where the benefits of this new technology will be advantageous in several aspects over established switching technologies [13].

The flight model of the switch matrix experiment including peripheral components of the ceramic modules is shown in Fig. 4 before integration into the satellite payload. The switch matrix module (1) is fed by two voltage-controlled oscillator modules (2), the routing inside the switch matrix is controlled by a *Field Programmable Gate Array* (FPGA) (5), and two diode driver modules (3) while the output ports are connected to microwave detectors (4). Each *voltage-controlled oscillator* (VCO) module is equipped with IHP-T208 and Hittite HMC633-LP4 VCOs, delivering two microwave signals between 17.2–19.2 GHz and 23.8–24.8 GHz (see also Fig. 5). The output power varies between 2 and 12 dBm and is fed into the switch matrix through coplanar waveguides with bond connections between the individual LTCC blocks (Fig. 6). Depending on the selected configuration of the 32 bipolar currents from the two diode driver modules, each microwave input signal is directed to one of four switch matrix outputs where power detectors provide an analogue voltage proportional to the microwave power. The combination of different sources and detectors enables a large number of combinations to be tested and allows for fault-redundant verification of the electrical functionality. The analogue voltages of detectors and status signals are multiplexed and converted into digital signals. In addition, temperature values are aquired at four different positions of the experiment for subsequent re-calibration of the detector readout values, for instance.

Since the satellite orbits the earth on a low orbit, there are times without direct line-of-sight connection. As the operational time segment approaches, the payload requires lists of commands and configurations to work autonomously. These commands have been pre-defined and allow for later on-board adjustments. Upon acquisition, the measured data are transferred to the ground control station in Neustrelitz during subsequent overflights. The experiment will be operated multiple times per week and two additional long term tests (24 hours) will be conducted during the mission. Malfunctions of the experiment or the satellite control circuitry can be detected by comparison to previous data, or to an identical redundant board that is also part of the payload, or to a reference board available on ground. Changes of the configuration and programms can be performed on a regular basis.

6 Analysis of typical data as measured in space

The properties of the reconfigurable switch matrix module depend, for instance, on frequency, incident power, temperature, and current through the PIN-diodes. The other microwave components have similar dependences. Therefore, calibration measurements had to be conducted for each module before mounting them onto the final circuit board. A change of temperature by 10 °C causes a pro-

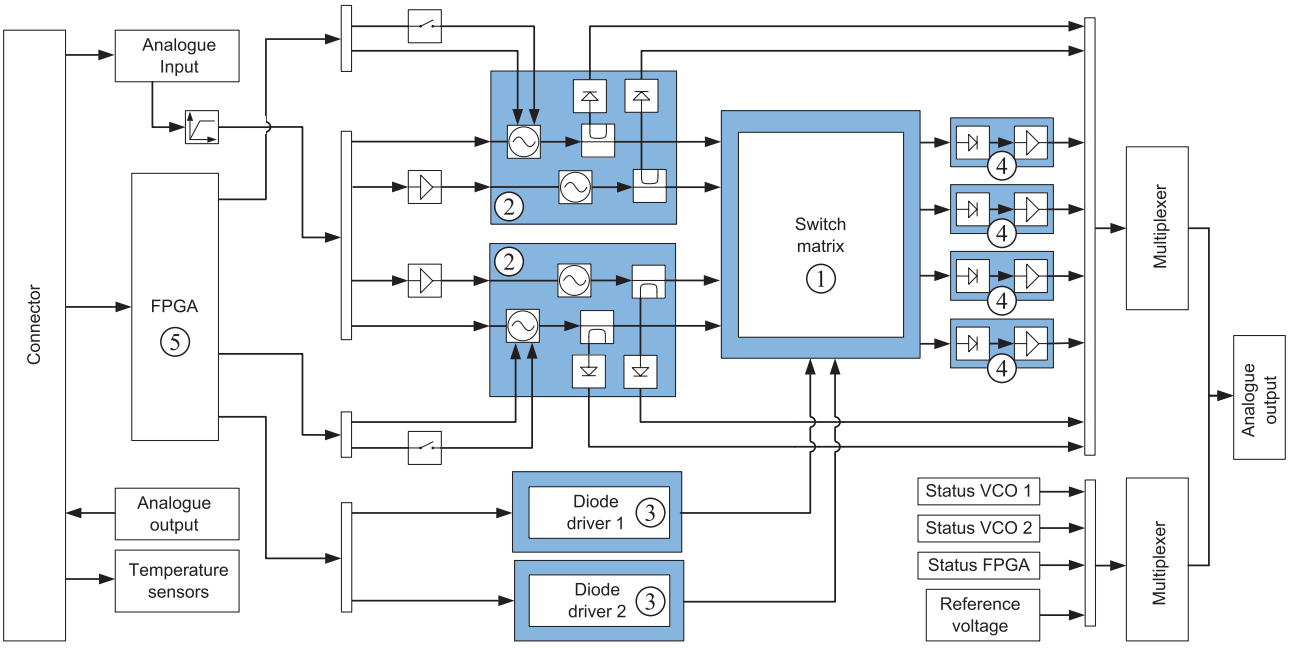

Fig. 6: Block diagram of the space experiment with the ceramic modules indicated in blue color. The switch matrix (1) is controlled by two diode driver modules (3) with digital inputs that provide bipolar currents for conditioning each of the 32 PIN-diodes. Two VCO modules (2) with two microwave sources provide the input signals for the switch matrix. Depending on the configuration, each input signal is routed to one output and detected (4). The experiment is controlled by a FPGA (5). The analogue output of the detectors as well as status voltages are multiplexed and converted to digital signals on a separate digital control board, common to all three experiments of the KERAMIS® payload.

nounced variation of the analogue voltage of the detector module, depicted in Fig. 7 as the difference between raw and calibrated data of up to 107 mV.

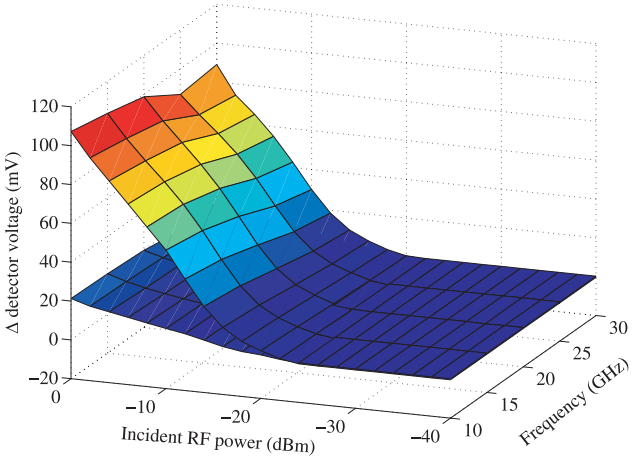

Fig. 7: Comparison of predicted detector voltage (low level, blue-shaded colours) and measured values (false-colour coded) as function of frequency and microwave-power. The behaviour at 10 °C was derived from the reference measurements at 22 °C and 0 °C. Without correction, the error would sum up to 107 mV while the compensation reduces the error from 10% to 2% for coarse reference sample points.

Applying a simple calibration algorithm proved very efficient to reduce the influence of temperature variations to a low-percentage level. The maximum remaining difference of 20 mV occurs at the highest output voltages of around 1 V. Incorporating measurements at intermediate temperatures reduces the error at arbitrary temperatures further, well below 1%. At calibration temperatures the error is ideally zero.

A MATLAB [14] program was used to calculate the bias points of the components under test, depending on digital settings and analogue values for voltages, frequencies, and temperatures. Current data sets are compared to previous results and should remain constant when no errors occur, as the drifts due to temperature and supply voltages are properly taken into account.

Knowledge of the transfer parameters of all individual components is essential for good repeatability of the measurements. For one VCO-module, the dependence of the output frequency on the control voltage is shown in Fig. 5 as an example. The tuning range of one type of oscillator was observed to be limited by the analogue input. However, it offered a coarse pre-adjustment through a four-bit digital input applied to the integrated varactor diodes.

7 Modular switch matrices of higher complexity

The complexity of switch matrix architectures of higher multiplicity increases with the number of input and output ports in a nonlinear way. The internal combination of ports via integrated switch circuits requires longer transmission lines, more layers and transitions, additional switches and bond connections, altogether causing higher insertion loss. Sustaining high path isolation around 70 dB requires careful design of transitions and shielded line configurations [15]. Due to the two-sided mounting of switch ICs, the manufacturing is complicated and would become even more challenging for more complex systems. A benefit of PIN-diodes in comparison with coaxial and waveguide switches is the fast switching speed, that can be applied for dynamic data routing. Other 2nd level interconnects such as LGA (land grid array) and BGA (ball grid array) may be applied to further improve the interface characterisitics [5] but the need to withstand mechanical stress prohibits large modules.

Further work has shown that the switch matrix can be miniaturised to outer dimensions of 25 mm × 25 mm, thereby reducing the required foot print to 34.4% by integrating the diode drivers [13]. This simplifies the carrier board as well and allows for a denser assembly (Fig. 8).

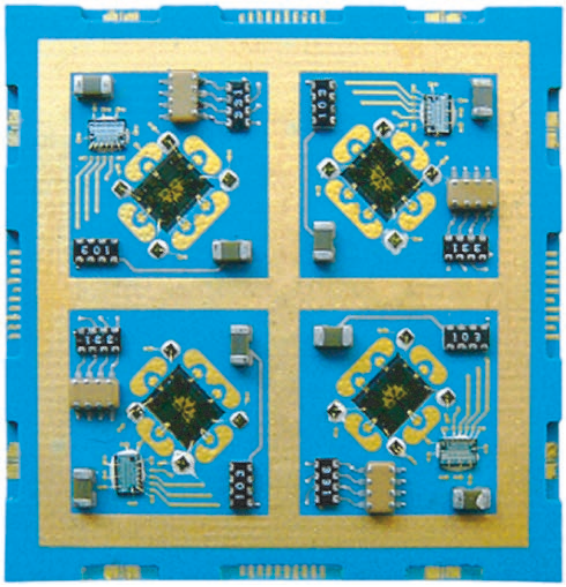

Fig. 8: Advanced version of the switch matrix (third generation), optimised with respect to higher device density and miniaturisation. Additionally, the module incorporates the diode drivers and reduces thereby the required footprint size to 34.4% (625 mm² compared to previously 1819 mm²).

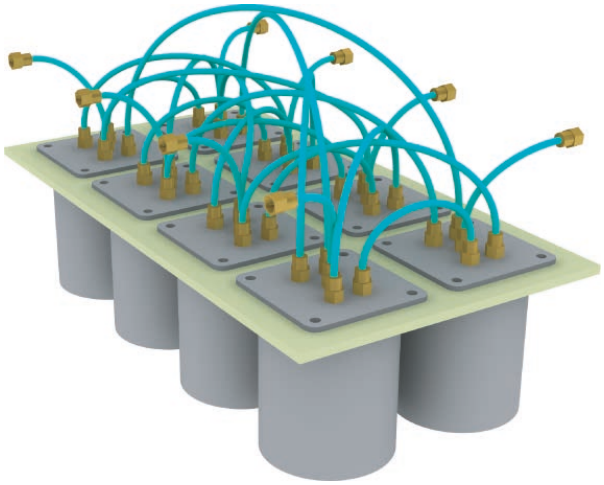

Fig. 9: Visualisation of a 4 × 4 switch matrix system build from conventional coaxial SP4T switches and the cables required for the interconnects. The function is comparable to the one of the ceramic module in Fig. 8.

The combination of eight convential coaxial SP4T-switches for the same 4 × 4 switch matrix complexity is depicted in Fig. 9 and has an estimated mass of 2000 g with a box volume of 6720 cm³ while the module acoording to Fig. 8 requires a volume of 12.5 cm³ with a mass of 20 g.

The architecture of a reconfigurable switch matrix of higher order would depend on the required multiplicity. Correspondingly, a modular approach would benefit from smaller modules (like a 4 × 4 RSM), providing a reasonable trade-off between complexity and flexibility. Different topologies such as the Beneš or Clos type [16] can be employed. In Fig. 10, one possible configuration of a 8 × 8 switch matrix is shown, requiring six of the previously described 4 × 4 switch matrix modules. A non-blocking behaviour (valid routing available independent of existing connections) can be achieved by choosing the appropriate topology (adding one additional switch in the centre stage).

The resulting S-parameters of such a modular approach correspond to the cascading of sequential stages, and the insertion loss of a single module approximately 4.5–6 dB increases by additional losses from the transmission lines and interconnects such as bond wires. To keep the insertion loss on a tolerable level, and comparable for all possible switching paths, gain-controlled amplifiers can be implemented in each module.

Compared to coaxial based switch matrices, the required mass and volume can be reduced drastically and additionally high switching speeds can be achieved. Especially as the control and power circuitry can be scaled very

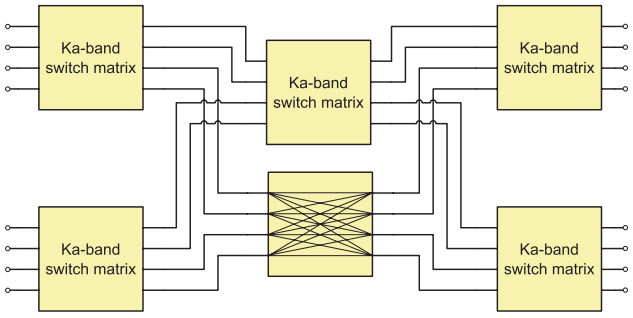

Fig. 10: The combination of 4 × 4 switch matrices enables higher complexities for the switch system with higher flexibility at the cost of additional line crossings and increased insertion loss. One of the modules depicts all possible connections between inputs and outputs of each identical switch matrix module.

effeciently for a higher number of switching modules with only a small increase of mass and volume. On the other hand the insertion loss is relatively high (5 dB compared to 1.4 dB at 20 GHz), the control circuits are more complex and power dissipation is much higher during static operation. The heat flow and thermal connection is therefore an integral part of the design process.

During manufacturing and testing the replacement of single modules with malfunction is advantageous over a single module of higher complexity. Additionally, the increased footprint size of single high-order switch matrices is expected to limit the mechanical robustness required for satellite applications [2].

Depending on the output configuration chosen, and the number of signals crossing from the top to the bottom level of a 8 × 8 switch matrix, a maximum of 9216 configurations fulfills the requirement. In case of an error at any of the 48 SP4T-switch-IC, one input signal can no longer be transmitted and the number of valid configuration drops. This effect depends on the position of the error and is more critical directly at the input and ouput ports.

8 Conclusions

We have developed a reconfigurable 4 × 4 Ka-band switch matrix to verify the circuit technology, package assembly, and qualification for space applications. For the integration into the TET-1 satellite and for an automated measurement, we developed a setup with additional components to prove the microwave properties of the switch matrix during the one year mission. The LTCC-technology enables the design and manufacturing of compact light-weight components with a comfortable degree of functional density and reliability. After a sucessful mission, a TRL-level of nine is achieved and enables a good utilisation of the described technology for future satellite payloads. The switch matrix allows for reduced mass and volume and is benefical in terms of costs and efficiency of modern satellites. Additionally, due to the fast electronic switching new applications become availabel (TDMA-schemes).

The robust design of the switch matrix experiment accounts for manufacturing tolerances and parameter calibration of all constituting components, as well as for a transparent analysis and verification of data.

The 4 × 4 switch matrix module can be used advantageously for higher complexities. In a separate project, a reconfigurable switch matrix module is presently under development for the German geostationary Heinrich Hertz satellite mission. The interconnects and control circuit are adapted to be used in communication satellite payloads.

Acknowledgement

This work has been funded by the German Federal Ministry of Economics and Technology (BMWi) under the project management of the German Aerospace Center (DLR, contract no. 50YB0622 and 50YB1112). We appreciate very much helpful support from A. Schwarz (RHe Microsystems GmbH, Radeberg) and D. Schwanke (Micro Systems Engineering GmbH, Berg) as well as K.-H. Drüe, M. Huhn, I. Koch, J. Trabert, and M. Zocher (TU Ilmenau).

Received: August 9, 2012.

References

[1] J. F. Trabert, M. A. Hein, J. Muller, R. A. Perrone, R. Stephan, and H. Thusf, "High functional density low-temperature co-fired ceramic modules for satellite communications," in *European Microwave Conference (EuMC)*, vol. 1, 2005, pp. 481–484.

[2] S. Humbla, J. Mueller, R. Stephan, D. Stoepel, J. F. Trabert, G. Vogt, and M. A. Hein, "Reconfigurable Ka-Band Switch Matrix for On-Orbit Verification," In *European Microwave Conference EuMC 2009*, 2009, pp. 610–613.

[3] S. Humbla, S. Kaleem, J. Müller, S. Rentsch, R. Stephan, D. Stöpel, J. Trabert, G. Vogt, and M. Hein, "On-orbit verification of a 4 × 4 switch matrix for space applications based on the low temperature co-fired ceramics technology," in *German Microwave Conference (GeMiC)*, 2012.

[4] A. Brokmeier, "LTCC-technology for miniaturised Ka-band frontends," In *European Microwave Conference (EuMC)*, vol. 2, 2005, pp. 631–634.

[5] T. Baras, M. C. Hermandez, and A. F. Jacob, "Electrical and thermomechanical evaluation of 2nd-level-interconnects for LTCC modules," in *International Microelectronics and Packaging Symposium (IMAPS)*.

[6] I. Wolff, "Design and Technology of Microwave and Millimeterwave LTCC Circuits and Systems," in *Proc. of the International Symposium on Signals, Systems and Electronics*, pp. 505–512.
[7] Min Miao, Xiaoqing Zhang, Yang Zhang, Shufang Xu, Lei Liang, and Zhensong Li, "Design and simulation of THz filters embedded in LTCC multi-layer substrate," in *International Conference of Electron Devices and Solid-State Circuits (EDSSC)*, 2011.
[8] "Homepage of the KERAMIS consortium." [Online]. Available: http://www.keramis.org
[9] S. Humbla, S. Rentsch, R. Stephan, D. Stöpel, J. F. Trabert, G. Vogt, and M. A. Hein, "Measured Frequency Dependent Complex Permittivity of Low Temperature Co-Fired Ceramic Microwave Modules," in *Microwave Materials and their Applications (MMA)*, 2010.
[10] S. Rentsch, "Bestimmung von Materialkennwerten zur Realisierung von Hoch- und Höchstfrequenzkomponenten in LTCC," Ilmenau, 2011.
[11] D. Stöpel, K.-H. Drüe, S. Humbla, M. Mach, G. Reppe, A. Rebs, M. Hein, T. Mache, G. Vogt, and J. Müller, "Fine-Line Structuring of Microwave Components on LTCC Substrates," in *Electronic System-Integration Technology Conference (ESTC)*, 2010, pp. 1–6.
[12] ECSS-E-ST-10C, "Space Engineering: System engineering general requirements," 2009.
[13] S. Kaleem, S. Humbla, S. Rentsch, J. Trabert, D. Stöpel, J. Müller, and M. A. Hein, "Compact Ka-band reconfigurable switch matrix with power failure redundancy," in *German Microwave Conference*, 2012, pp. 1–4.
[14] "Homepage of The MathWorks, Inc. MATLAB." [Online]. Available: http://www.mathworks.com/products/matlab
[15] J. F. Trabert and M. A. Hein, "Impedanzkontrolliertes koplanares Wellenleitersystem zur dreidimensionalen Verteilung von Signalen hoher Bandbreite," Patent 10 2007 028 799.4, 2008.
[16] I. Gragopoulos and F.-N. Pavlidou, "A new evaluation criterion for Clos- and Benes-type rearrangeable switching networks," *IEEE Transactions on Communications*, vol. 45, no. 1, pp. 119–126, 1997.